HHS Public Access

Author manuscript

Ultrasound Med Biol. Author manuscript; available in PMC 2020 January 01.

Published in final edited form as:

Ultrasound Med Biol. 2019 January ; 45(1): 129–136. doi:10.1016/j.ultrasmedbio.2018.08.023.

Testing different combinations of acoustic pressure and doses of quinolinic acid to induce focal-neuron loss in mice using transcranial low-intensity focused ultrasound

Yanrong Zhang[1,2], **Chengde Liao**[2,3], **Haibo Qu**[2,4], **Siqin Huang**[2,5], **Hong Jiang**[2,6], **Haiyan Zhou**[2,7], **Emily Abrams**[8], **Frezghi G. Habte**[9], **Li Yuan**[2], **Edward H. Bertram**[10], **Kevin S. Lee**[11], **Kim Butts Pauly**[12], **Paul S. Buckmaster**[8], and **Max Wintermark**[2]

[1]Department of Ultrasound, Wuhan Children's Hospital (Wuhan Maternal and Child Healthcare Hospital), Tongji Medical College, Huazhong University of Science and Technology, China

[2]Department of Radiology, Neuroradiology Section, Stanford, CA

[3]Department of Radiology, The Third Affiliated Hospital of Kunming Medical University, The Tumor Hospital of Yunnan Province, Kunming, Yunnan, China

[4]Department of Medical Imaging, West China Second University Hospital, Sichuan University, Chengdu, Sichuan 610041, China

[5]Chongqing Medical University, Traditional Chinese Medicine College, Chongqing, China

[6]Department of Neurology, Peking University of People's Hospital, Beijing, China

[7]The Acupuncture and Tuina School/The 3rd Teaching Hospital, Chengdu University of Traditional Chinese Medicine, No. 37, Shierqiao Street, Chengdu, Sichuan 610075, China

[8]Stanford University, Department: Comparative Medicine, Stanford, CA

[9]Department of Radiology, Molecular Imaging Program at Stanford, CA

[10]Department of Neurology, University of Virginia, Charlottesville, Virginia, USA

[11]Departments of Neuroscience and Neurosurgery, and Center for Brain Immunology and Glia, University of Virginia, Charlottesville, Virginia, USA

[12]Department of Radiology, Stanford University, Stanford, CA, USA

Abstract

The goal of this study was to test different combinations of the acoustic pressure and doses of quinolinic acid (QA) to produce a focal neuronal lesion in the murine hippocampus without causing unwanted damage to adjacent brain structures. Sixty male CD-1 were divided into 12

Address for correspondence and reprint requests: Max Wintermark, MD, Stanford University School of Medicine, Department of Radiology, Neuroradiology Section, 300 Pasteur Drive, Grant - S047, Stanford, CA 94305, 650-723-7426 (phone), 650-498-53474 (fax), max.wintermark@gmail.com.

groups receiving the following treatments: MRgFUS at high (0.67 MPa), medium (0.5 MPa), and low acoustic peak negative pressure (0.33 MPa), and QA at high (0.012 mmol), medium (0.006 mmol) and low (0.003 mmol) dosage. Neuronal loss occurred only when MRgFUS with adequate acoustic power (0.67MPa or 0.5 MPa) was combined with QA. When the highest acoustic power was delivered, the animals showed larger lesion size than those treated with medium acoustic power, but 2 mice showed evidence of bleeding. When the intermediate acoustic power utilized, medium and high dosages of QA produced larger lesions than that of the low dosage produced.

Keywords

Blood–brain barrier; Epilepsy; Hippocampus; Magnetic resonance-guided focused ultrasound; Quinolinic acid; Transcranial drug delivery

Introduction

In the United States, 1 of 26 people will develop epilepsy at some point in their lifetime (England et al. 2012). In approximately two-thirds of people with epilepsy, seizures can be successfully controlled with currently-available antiepileptic drugs (AEDs), leaving one-third with uncontrolled epilepsy. Patients who are refractory to various combinations of anti-epileptic drugs become candidates for surgical resection of the site of seizure genesis. For instance, resective surgery in temporal lobe epilepsy, the most common type of epilepsy in adults is quite effective, improving epilepsy in upwards of 70% of patients (Wiebe et al. 2001). However, it is highly invasive and requires the removal of substantial amounts of cortical tissue. Persistent functional deficits in memory, language comprehension and visual processing may occur (Helmstaedter et al. 2004). Moreover, complications can include bleeding, infection, thrombi, stroke, seizures, swelling of the brain and nerve damage (McClelland, 3rd et al. 2011).

Alternatives to conventional epilepsy surgery include minimally invasive laser ablation (Willie et al. 2014), and non-invasive radio-surgery (Quigg et al. 2008). Magnetic resonance (MR)-guided focused ultrasound (MRgFUS) is also under development as another non-invasive surgical tool for epilepsy and other disorders (Martin et al. 2009; Elias et al. 2013; Monteith et al. 2013). High intensity MRgFUS is a non-invasive method for thermal ablation of targeted tissue, and it is approved by the Food and Drug Administration for the treatment of symptomatic uterine fibroids (Hesley et al. 2013), painful bone metastasis (Yeo et al. 2015), osteoid osteoma (Napoli et al. 2017), and essential tremor (Elias et al. 2013). This technology uses directional ultrasound waves that achieve a precise focus pinpointing a small target, providing a therapeutic effect by raising the temperature sufficiently to destroy the target without producing substantial damage to the surrounding tissue. MR imaging is used to define the target and surrounding critical anatomic structures, and to assess treatment effects, including the volume of non-perfused tissue after ablation. One limitation of high intensity MRgFUS is that, in order to perform an ablation of a specific brain region, the deposition of a significant amount of energy to this region is required. This critical amount of energy deposition can be achieved only when the gain of the focused beam is high enough to overcome the dissipation effect of the skull. The resulting treatment envelope includes

tissues located a greater distance from the skull (e.g., thalamus), whereas structures located nearer to bone (e.g., hippocampus) are more challenging to treat (Hynynen et al. 1999; Aubry et al. 2003; Lu et al. 2006; Marquet et al. 2009; Pinton et al. 2012).

An alternative approach is to utilize low intensity MgFUS in combination with systemically-administered microbubbles. This produces a transient/reversible opening of the blood brain barrier (BBB), allowing the delivery of BBB-impermeable compounds to the targeted area. The lower intensity sonication does not directly produce tissue damage (Hynynen et al. 2001), and has the added benefit of expanding the treatment envelope beyond midline brain structures (Konofagou 2012). In a previous study, we utilized this approach to focally deliver a neurotoxin with poor intrinsic BBB permeability (quinolinic acid [QA]) to produce a targeted, non-invasive disconnection of brain circuitry in the hippocampus (Zhang et al. 2016). The goal of the current study was to extend these findings by testing different combinations of acoustic power and doses of QA to produce a focal lesion with neuron loss in the murine hippocampus without causing unwanted damage to adjacent brain structures.

MATERIALS AND METHODS

Study design

The animal protocol was approved by the Stanford University Administrative Panel on Laboratory Animal Care (APLAC). All experiments were conducted in accordance with the National Institutes of Health's Guide for the Care and Use of Laboratory Animals.

Male CD-1 mice (Charles River Laboratories, Wilmington, MA, USA), 6–8 wk of age, were divided into 12 groups receiving the following treatments: MRgFUS at high (0.67 MPa), medium (0.5 MPa), and low derated peak negative pressure (0.33 MPa), and QA at high (0.012 mmol), medium (0.006 mmol) and low (0.003 mmol) dosage, including a saline control group. QA (Santa Cruz Biotechnology, Dallas, TX, USA) was dissolved in saline (10 mg/mL). QA was intraperitoneally injected every 6 hours for a total of four doses within 24 hours of the MRgFUS session. A study of the pharmacodynamics of intravenous injection of QA, using isotope-labeled tryptophan as a precursor for the in vivo production of labeled QA in rabbits, found the half-life of QA to be about six hours (Boni et al. 1991). The half-life of single dose of QA is twice as long as for an intravenous injection when it was injected intraperitoneally or subcutaneously. By injecting QA multiple times, every 6 hrs for 24 hrs prior to treatment, we were able to get a relatively stable plasma concentration of QA during the window of BBB opening, taking optimal advantage of this window. The timing of QA delivery with respect to the MRgFUS treatment was based on the dynamic of BBB opening described in previous reports (Hynynen et al. 2001) (Konofagou et al. 2012). All mice received Definity® Microbubbles (mean diameter range: 1.1–3.3 μm, mean concentration of 1.2 × 10^10 bubbles per mL, warmed up to room temperature according to manufacturer's instruction (Helfield et al. 2012), diluted by 1:20 using 1× phosphate-buffered saline (PBS), 300 μL/kg, Lantheus Medical Imaging, MA, USA) delivered via the tail vein just before sonication. During the procedure, mice were anesthetized with isoflurane (4% induction and 2% maintenance). All animals were euthanized 7 days post-MRgFUS treatment.

Magnetic resonance-guided focused ultrasound system

The MRgFUS system (Image Guided Therapy, Pessac, France) was configured as described previously (Zhang et al. 2015; Zhang et al. 2016). It includes an MR-compatible, pre-focused, eight-element annular array, 1.5-MHz transducer (spherical radius = 20+/−2 mm, active diameter=25 mm [focal ratio =0.8], Imasonic, Voray sur l'Ognon, France), which was connected to a phased array generator and radiofrequency power amplifier. An MR-compatible motorized positioning stage was used to move the transducer in the rostral-caudal and medial-lateral directions. The focus was moved along the direction of the ultrasound beam by electronic steering. The membrane in front of the transducer was filled with degassed water and inflated to ensure good ultrasonic coupling between the membrane and the head of the animal.

For sonication, the animals were placed in a prone position and maintained in this position using a bite bar and ear bars (Fig. 1). The scalp hair was shaved and removed with depilatory cream. Acoustic gel was applied between the transducer and skin. A catheter was inserted into the tail vein. MRI was performed using a 3-T preclinical system (MR Solutions, Guildford, Surrey, UK).

Target localization and sonication

To target the left hippocampus, the FUS transducer was laterally moved 3 mm to the left of the sagittal suture and 2 mm anterior of the lambdoid suture, as described previously (Chen et al. 2014). Treatments included up to five points of sonication. The sonication zones were moved slightly rostral-caudally and laterally in the vicinity of the identified target (1.5 MHz, pulse duration 20-ms, duty cycle of 2%, 1-Hz pulse repetition frequency, 120-s duration per sonication, these parameters have been applied to open the BBB successfully in Zhang et al's study {Zhang et al, 2016}, the acoustic pressure was the one to which the hippocampus would be exposed).

MR imaging for BBB opening and injury after sonication

In order to achieve quantitative hemodynamic measurements of blood-brain barrier opening and permeability, a bolus of gadobenate dimeglumine (Multihance, Bracco Diagnostics Inc. Monroe Township, NJ 08831, USA) was injected and dynamic contrast enhancement (DCE) MR imaging was performed immediately, Day 1, and Day 7 post treatment (TR/ TE = 65/3 ms, average = 2, field of view 25 mm, flip angle 35°, matrix size=68×128, slice thickness=1.3 mm).

Post-contrast T1-weighted imaging (TR/ TE =720/11 milliseconds, 4 averages, field of view=25 mm, matrix size=248×512, slice thickness=0.6 mm) was obtained to depict the area of contrast-enhancement in the hippocampus.

T2*- weighted gradient echo imaging (repetition time/echo time [TR/TE]=391/20 ms, flip angle 20°, 3 averages, field of view 25 mm, matrix size=256×256, slice thickness 0.8 mm) was performed immediately after sonication to evaluate possible hemorrhagic complications.

To assess resulting lesions during the follow-up period, T2-weighted fast spin echo (FSE) images (TR/TE=4800/85 ms, 1 average, field of view=25 mm, matrix size=240×256, slice

thickness 1.2 mm) were acquired at three time points: immediately, Day 1 and Day 7 after sonication.

Image processing

The images were analyzed using the DICOM viewer Horos, and the blood-to-brain-transfer constants (referred to as Ktrans in the remainder of the text) maps were computed from DCE MR imaging with the extended Tofts model using the plugin software IB DCE (Imaging Biometrics, Elm Grove, WI, USA).

On T1-post contrast images, one set of regions of interest (ROIs) was drawn to include the enhanced area, and another set of ROIs to include the mirrored contralateral area, and a post-gadolinium T1 intensity ratio was calculated. The areas of these ROIs were recorded, and Ktrans values in these ROIs were also recorded.

Tissue preparation and staining

Immediately after MR imaging at 7 days post sonication, mice were euthanized (>100 mg/kg pentobarbital, i.p.) and perfused through the left ventricle at 15 mL/min for 1 min with 0.9% NaCl and for 30 min with 4% formaldehyde in 0.1 M phosphate buffer (PB, pH 7.4). Brains were post-fixed overnight at 4°C and then transferred into 30% (w/v) sucrose in phosphate buffer. After equilibrating in the 30% sucrose solution, the brains were sectioned coronally with a sliding microtome set at 40 μm. Serial sections were collected in 30% ethylene glycol and 25% glycerol in 50 mM PB and stored at −20˚C until use. Series of adjacent sections were processed for Nissl staining to show the Nissl body (the large granulars of rough endoplasmic reticulum) and visualize the neurons in the brain. Prussian blue iron stain, which can be used to demonstrate ferric iron and ferritin through Prussian blue reaction was performed for mice with bleeding on MR images.

Statistical analysis

We used median and interquartile range (IQR) for our descriptive statistics. The nonparametric Kruskal-Wallis test was used to assess differences in BBB permeability among different groups. The Mann-Whitney U test was used to evaluate differences in other outcomes between groups. Multiple comparisons were adjusted using a bonferroni correction. Probability values of less than 0.05 were considered statistically significant. The statistical software IBM SPSS version 22 was used for the statistical analyses.

RESULTS

Evolution of MRI changes over time

Immediately after sonication, 51 of 60 mice showed enhancement on post contrast T1-weighted imaging, consistent with opening of the BBB. Nine of the 20 mice treated with low acoustic power did not show enhancement on post contrast T1-weighted images. Ten of the 20 mice treated with high acoustic power and 4 of the 20 mice treated with medium acoustic power exhibited edema (i.e. enhanced signal on T2-weighted images), while the rest of the mice did not show change on the T2-weighted images obtained immediately after sonication

(Table 1). GRE imaging did not show evidence of bleeding at the immediate post-sonication time point (Fig. 2)

One day post sonication, both post contrast T1-weighted imaging and DCE showed BBB-opening in all of the mice treated with high and medium acoustic power and in 5 of the 20 mice sonicated with low acoustic power. The remaining 15 mice from the low acoustic power groups did not show any apparent BBB-opening. Five mice out of the 20 from the high acoustic power groups showed high signal on T2-weighted imaging. The remaining 15 mice did not show change on T2-weighted and GRE imaging (Table 1). Examples of a mouse exhibiting enhanced T2 signal (Fig. 2A), and a mouse not exhibiting enhanced T2 signal at 24 hours (Figure 2B) are shown in Figure 2.

Seven days post sonication, no evidence of BBB opening was observed on the post-contrast T1-weighted imaging or with DCE. Only 2 animals exhibited evidence of microbleeds based on GRE: one mouse treated with high ultrasound power and the high dose of QA and one mouse treated with high ultrasound power and saline. The remaining 18 mice did not show changes on T2-weighted and GRE imaging. (Regarding Fig. 2)

BBB opening extent immediately after FUS exposure on MRI

The mice treated with high acoustic power showed a greater post-gadolinium T1 intensity ratio between the sonicated area and the contralateral parenchyma (P=0.045 versus Medium FUS group, P=0.042 versus Low FUS group) and greater Ktrans values compared to those treated with medium (P=0.006) and low acoustic power (P<0.001). The enhancing area of the mice treated with high and medium acoustic power was larger compared to that from the mice treated with low acoustic power (Table 2).

Histologic evidence of QA-induced damage at D7 post sonications

Figure 3 shows images of Nissl-stained tissue sections from 3 mice treated with the same dosage of QA (0.012 mmol), but receiving one of three intensities of acoustic power. Clear loss of neurons in the target area of the hippocampus can be observed in the animals receiving FUS at high or medium acoustic powers.In contrast, the animal receiving FUS at a low acoustic power did not display cell loss. (Fig. 3)

The mice administered high acoustic power from QA-treated groups showed larger lesion size than those treated with medium acoustic power, but again there were 2 mice showing evidence of bleeding, one from the high-FUS+ high-QA group, and another one from high FUS+ saline group. When sonicated with medium acoustic power, the mice injected with high or medium dosage of QA showed larger lesions than the mice injected with the low dosage of QA (Table 3).

DISCUSSION

The efficacy of therapeutic candidates targeting neurologic disorders is severely hampered by the existence of a BBB that impedes the access of most pharmacologic agents to the central nervous system. MRgFUS has emerged as an effective, non-invasive treatment method to open the BBB in a targeted, transient, and non-destructive manner, increasing its

permeability to large molecules into the brain. In preclinical studies, BBB opening using MRgFUS has been used to deliver chemotherapeutic agents (Fan et al. 2016), antibodies (Alecou et al. 2017), stem cells (Burgess et al. 2011), and targeted genes (Mead et al. 2016). Previously, we have shown that, combined with systematically administered microbubbles and intraperitoneally injected QA, low-intensity MRgFUS (1.5 MHz, 0.69MPa) opened the BBB successfully and non-invasively induced focal neuron loss in the rat hippocampus area (Zhang et al. 2016).

Systemic administration of QA is generally well tolerated. Single intravenous injections of 450 mg/kg QA do not produce neuronal degeneration in the hippocampus (Foster et al. 1984). Moreover, repeated intraperitoneal injections of 60 mmol/d for 8 d were well tolerated but produced some evidence of ultrastructural modification of the cells in the hypothalamus (Beskid et al. 1997). This general lack of neurotoxicity even after the administration of very high systemic dosages has been ascribed to the BBB impermeability of QA through the BBB (Foster et al. 1984). In our initial study on rats, we selected an intraperitoneal dose of 0.06 mmol per day for the rats 5–6 weeks of age (120–150 grams body weight), which is a dosage 1000 times weaker than that used in a previous study (Beskid et al. 1997). In the current study, we examined mice 5–6 weeks of age (20–25 grams body weight), which represents approximately 1/5 of the weight of the rats utilized in our previous study. Accordingly, 0.012mmol of QA (i.e. 1/5 of the dose injected to rats in the previous study) was selected for a starting dosage for treatment in the current study. In addition, a dose de-escalation protocol involving 0.006mmol and 0.003mmol was tested. A parametric assessment of the effect of acoustic power was also tested by sonicating the mice at acoustic powers of 0.67MPa, 0.5MPa, or 0.33MPa. Acoustic powers above and below 0.5 MPa were chosen because 0.46MPa has been shown to be the threshold for inertial cavitation of Definity microbubbles, and the threshold for BBB opening is within the range of 0.15–0.30 MPa rarefactional pressure amplitude (Baseri et al. 2010). Our study demonstrated that 0.33 MPa opened BBB in more than 50% (11/20) of the mice, and that all of the mice treated with 0.5MPa or 0.67 MPa showed successful opening of the BBB, which is consistent with the results from B. Baseri et al's study.

Microbubbles play a critical role in catalyzing the FUS-induced BBB-opening effect. The maximum dose of the microbubble contrast agent Definity is 20 μL/kg in humans, as recommended by the manufacturer. Literature shows that preclinical studies on BBB opening used various dose of Definity. In Baseri et al's study(Baseri et al. 2010), 50μl of original concentration per kilogram of mouse body mass was used. In Wang et al's study (Wang et al. 2014), 1 μl/g diluted microbubbles (6×10^8 number per mL) was used, which is higher than our dose of microbubbles in current and previous study (Zhang et al. 2016).

In most of our treated cases, the BBB was still opening at 24 hrs post sonication. The reports from different groups have shown various durations of BBB opening by FUS, which probably relates to individual acoustic settings, as well as type and dosage of microbubbles. In Hynynen and coauthors' study on rabbits, the BBB opening could last up to 72 hours (Hynynen et al. 2001), In Samiotaki at al's study, the volume of BBB opening was found to increase with both pressure and microbubble diameter. The duration required for closing was found to be proportional to the degree of opening on the day of opening, and ranged from 24

h, for the smaller microbubbles, to 5 days at high peak-rarefactional pressures (Samiotaki et al. 2012). Shorter BBB opening duration was found in O'Reilly et al's study, where T1-weighted imaging revealed that BBB in 9 of 10 hemispheres were fully closed by 6 hours after focused US. BBB in the remaining hemisphere was fully closed by 24 hours (O'Reilly et al. 2017).

The current findings indicate that MRgFUS together with microbubbles opened the BBB in the area of sonication regardless of whether saline or QA was administered. However, neuronal loss occurred only when MRgFUS with adequate acoustic power (0.67MPa or 0.5 MPa) was combined with QA. When the highest acoustic power (0.67MPa) was delivered, the size of the lesion produced did not depend on the dosage of QA that was administered, which means the highest acoustic pressure also leads to brain tissue damage including neuron loss and hemorrhage. In contrast, the dosage of QA did affect lesion size when the intermediate acoustic power (0.5MPa) utilized, with medium and high dosages of QA producing larger lesions than the low dosage. There is probably a threshold/ceiling effect. Once a certain amount of QA makes it to the brain tissue, the sought effect occurs. If more QA gets there, the same effect occurs. Together, these findings demonstrate that both the intensity of acoustic power delivered and the dosage of QA influence on the resultant neuronal damage. One limitation of our study is that the actual concentration of the QA delivered into the tissue and the delivery efficiency were not measured, Also, the lesion size necessary to elicit a therapeutically relevant effect will need to be determined in a future study.

CONCLUSIONS

This study refines our knowledge for producing neuronal lesions using MRgFUS combined with QA, by defining the optimal combination of rarefactional pressure amplitude at 0.5MPa and QA dosage (0.006 mmol per injection) in mice under the conditions of 1.5 MHz, pulse duration 20-ms, duty cycle of 2%, 1-Hz pulse repetition frequency, 120-s duration per sonication. These parameters can be used in future work on the treatment study with animal models such as mice with epilepsy.

ACKNOWLEDGMENTS

This work was supported by NIH grants R01 CA217953-01 and R01NS102194.

REFRENCES

Alecou T, Giannakou M and Damianou C "Amyloid beta Plaque Reduction With Antibodies Crossing the Blood-Brain Barrier, Which Was Opened in 3 Sessions of Focused Ultrasound in a Rabbit Model." J Ultrasound Med 2017; 36(11): 2257–2270. [PubMed: 28543446]

Aubry JF, Tanter M, Pernot M, Thomas JL and Fink M "Experimental demonstration of noninvasive transskull adaptive focusing based on prior computed tomography scans." J Acoust Soc Am 2003; 113(1): 84–93. [PubMed: 12558249]

Baseri B, Choi JJ, Tung YS and Konofagou EE "Multi-modality safety assessment of blood-brain barrier opening using focused ultrasound and definity microbubbles: a short-term study." Ultrasound Med Biol 2010; 36(9): 1445–1459. [PubMed: 20800172]

Beskid M, Rozycka Z and Taraszewska A “Quinolinic acid: effect on the nucleus arcuatus of the hypothalamus in the rat (ultrastructural evidence).” Exp Toxicol Pathol 1997; 49(6): 477–481. [PubMed: 9495649]

Boni RL, Heyes MP, Bacher JD, Yergey JA, Ji XD, Abramson FP and Markey SP “Stable isotope-labeled tryptophan as a precursor for studying the disposition of quinolinic acid in rabbits.” Adv Exp Med Biol 1991; 294: 481–484. [PubMed: 1837688]

Burgess A, Ayala-Grosso CA, Ganguly M, Jordao JF, Aubert I and Hynynen K “Targeted delivery of neural stem cells to the brain using MRI-guided focused ultrasound to disrupt the blood-brain barrier.” PLoS One 2011; 6(11): e27877. [PubMed: 22114718]

Chen H and Konofagou EE “The size of blood-brain barrier opening induced by focused ultrasound is dictated by the acoustic pressure.” J Cereb Blood Flow Metab 2014; 34(7): 1197–1204. [PubMed: 24780905]

Elias WJ, Huss D, Voss T, Loomba J, Khaled M, Zadicario E, Frysinger RC, Sperling SA, Wylie S, Monteith SJ, Druzgal J, Shah BB, Harrison M and Wintermark M “A pilot study of focused ultrasound thalamotomy for essential tremor.” N Engl J Med 2013; 369(7): 640–648. [PubMed: 23944301]

England MJ, Liverman CT, Schultz AM and Strawbridge LM “Epilepsy across the spectrum: promoting health and understanding. A summary of the Institute of Medicine report.” Epilepsy Behav 2012; 25(2): 266–276. [PubMed: 23041175]

Fan CH, Cheng YH, Ting CY, Ho YJ, Hsu PH, Liu HL and Yeh CK “Ultrasound/Magnetic Targeting with SPIO-DOX-Microbubble Complex for Image-Guided Drug Delivery in Brain Tumors.” Theranostics 2016; 6(10): 1542–1556. [PubMed: 27446489]

Foster AC, Miller LP, Oldendorf WH and Schwarcz R “Studies on the disposition of quinolinic acid after intracerebral or systemic administration in the rat.” Exp Neurol 1984; 84(2): 428–440. [PubMed: 6232146]

Helfield BL, Huo X, Williams R and Goertz DE “The effect of preactivation vial temperature on the acoustic properties of Definity.” Ultrasound Med Biol 2012; 38(7): 1298–1305. [PubMed: 22502892]

Helmstaedter C, Van Roost D, Clusmann H, Urbach H, Elger CE and Schramm J “Collateral brain damage, a potential source of cognitive impairment after selective surgery for control of mesial temporal lobe epilepsy.” J Neurol Neurosurg Psychiatry 2004; 75(2): 323–326. [PubMed: 14742620]

Hesley GK, Gorny KR and Woodrum DA “MR-guided focused ultrasound for the treatment of uterine fibroids.” Cardiovasc Intervent Radiol 2013; 36(1): 5–13. [PubMed: 22453202]

Hynynen K, McDannold N, Vykhodtseva N and Jolesz FA “Noninvasive MR imaging-guided focal opening of the blood-brain barrier in rabbits.” Radiology 2001; 220(3): 640–646. [PubMed: 11526261]

Hynynen K and Sun J “Trans-skull ultrasound therapy: the feasibility of using image-derived skull thickness information to correct the phase distortion.” IEEE Trans Ultrason Ferroelectr Freq Control 1999; 46(3): 752–755. [PubMed: 18238476]

Konofagou EE “Optimization of the ultrasound-induced blood-brain barrier opening.” Theranostics 2012; 2(12): 1223–1237. [PubMed: 23382778]

Konofagou EE, Tung YS, Choi J, Deffieux T, Baseri B and Vlachos F “Ultrasound-induced bloodbrain barrier opening.” Curr Pharm Biotechnol 2012; 13(7): 1332–1345. [PubMed: 22201586]

Lu M, Wan M, Xu F, Wang X and Chang X “Design and experiment of 256-element ultrasound phased array for noninvasive focused ultrasound surgery.” Ultrasonics 2006; 44 Suppl 1: e325–330. [PubMed: 16949119]

Marquet F, Pernot M, Aubry JF, Montaldo G, Marsac L, Tanter M and Fink M “Non-invasive transcranial ultrasound therapy based on a 3D CT scan: protocol validation and in vitro results.” Phys Med Biol 2009; 54(9): 2597–2613. [PubMed: 19351986]

Martin E, Jeanmonod D, Morel A, Zadicario E and Werner B “High-intensity focused ultrasound for noninvasive functional neurosurgery.” Ann Neurol 2009; 66(6): 858–861. [PubMed: 20033983]

McClelland S, 3rd, Guo H and Okuyemi KS "Population-based analysis of morbidity and mortality following surgery for intractable temporal lobe epilepsy in the United States." Arch Neurol 2011; 68(6): 725729.

Mead BP, Mastorakos P, Suk JS, Klibanov AL, Hanes J and Price RJ "Targeted gene transfer to the brain via the delivery of brain-penetrating DNA nanoparticles with focused ultrasound." J Control Release 2016; 223: 109–117. [PubMed: 26732553]

Monteith S, Sheehan J, Medel R, Wintermark M, Eames M, Snell J, Kassell NF and Elias WJ "Potential intracranial applications of magnetic resonance-guided focused ultrasound surgery." J Neurosurg 2013; 118(2): 215–221. [PubMed: 23176339]

Napoli A, Bazzocchi A, Scipione R, Anzidei M, Saba L, Ghanouni P, Cozzi DA and Catalano C "Noninvasive Therapy for Osteoid Osteoma: A Prospective Developmental Study with MR Imaging-guided High-Intensity Focused Ultrasound." Radiology 2017; 285(1): 186–196. [PubMed: 28590796]

O'Reilly MA, Hough O and Hynynen K "Blood-Brain Barrier Closure Time After Controlled Ultrasound-Induced Opening Is Independent of Opening Volume." J Ultrasound Med 2017; 36(3): 475–483. [PubMed: 28108988]

Pinton G, Aubry JF, Bossy E, Muller M, Pernot M and Tanter M "Attenuation, scattering, and absorption of ultrasound in the skull bone." Med Phys 2012; 39(1): 299–307. [PubMed: 22225300]

Quigg M and Barbaro NM "Stereotactic radiosurgery for treatment of epilepsy." Arch Neurol 2008; 65(2): 177–183. [PubMed: 18268185]

Samiotaki G, Vlachos F, Tung YS and Konofagou EE "A quantitative pressure and microbubble-size dependence study of focused ultrasound-induced blood-brain barrier opening reversibility in vivo using MRI." Magn Reson Med 2012; 67(3): 769–777. [PubMed: 21858862]

Wang S, Samiotaki G, Olumolade O, Feshitan JA and Konofagou EE "Microbubble type and distribution dependence of focused ultrasound-induced blood-brain barrier opening." Ultrasound Med Biol 2014; 40(1): 130–137. [PubMed: 24239362]

Wiebe S, Eliasziw M and Matijevic S "Changes in quality of life in epilepsy: how large must they be to be real?" Epilepsia 2001; 42(1): 113–118. [PubMed: 11207794]

Willie JT, Laxpati NG, Drane DL, Gowda A, Appin C, Hao C, Brat DJ, Helmers SL, Saindane A, Nour SG and Gross RE "Real-time magnetic resonance-guided stereotactic laser amygdalohippocampotomy for mesial temporal lobe epilepsy." Neurosurgery 2014; 74(6): 569–584; discussion 584–565. [PubMed: 24618797]

Yeo SY, Elevelt A, Donato K, van Rietbergen B, Ter Hoeve ND, van Diest PJ and Grull H "Bone metastasis treatment using magnetic resonance-guided high intensity focused ultrasound." Bone 2015; 81: 513–523. [PubMed: 26325304]

Zhang Y, Aubry JF, Zhang J, Wang Y, Roy J, Mata JF, Miller W, Dumont E, Xie M, Lee K, Zuo Z and Wintermark M "Defining the optimal age for focal lesioning in a rat model of transcranial HIFU." Ultrasound Med Biol 2015; 41(2): 449–455. [PubMed: 25542495]

Zhang Y, Tan H, Bertram EH, Aubry JF, Lopes MB, Roy J, Dumont E, Xie M, Zuo Z, Klibanov AL, Lee KS and Wintermark M "Non-Invasive, Focal Disconnection of Brain Circuitry Using Magnetic Resonance-Guided Low-Intensity Focused Ultrasound to Deliver a Neurotoxin." Ultrasound Med Biol 2016; 42(9): 2261–2269. [PubMed: 27260243]

Fig. 1. Experimental apparatus and post contrast T1-weighted image immediately after sonication.

A: A 3T MRI scanner was used to detect the BBB-opening after sonication. B: FUS system, a 1.5-MHz transducer in brown rests upon the top of the rodent head and can move in X-Y planes, and be focused in the Z axis. C: Post contrast T1-weighted image immediately post sonication; enhancement of the left ventral hippocampus area (black arrows) indicated BBB opening.

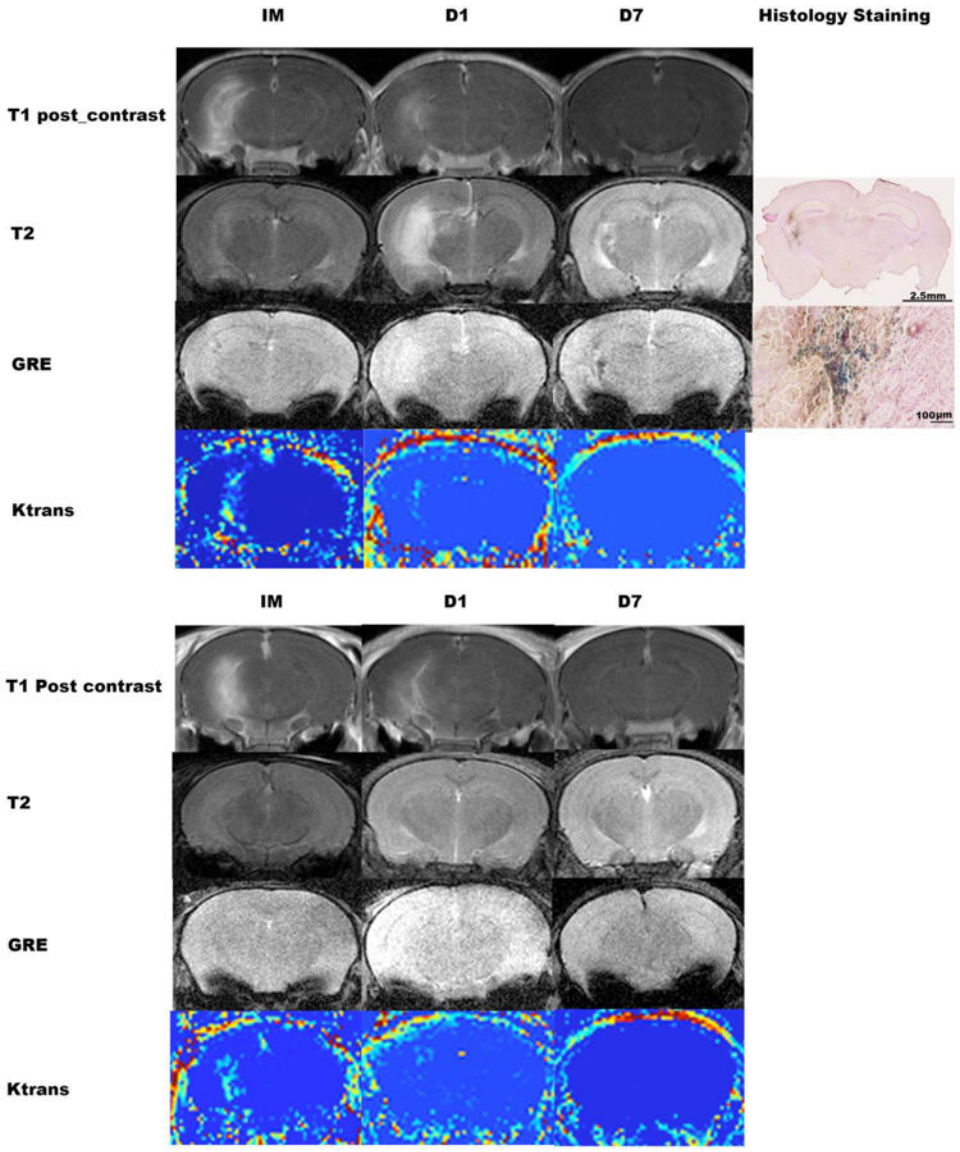

Fig. 2. Time course of MRI changes from 2 example mice treated with high acoustic power, and Prussian blue staining images from the one animal showing bleeding on GRE.

A: Immediately (IM) after sonication, both T1-post contrast imaging and DCE imaging showed BBB opening in the target area, and T2-weighted images showed mildly increased signal in the area with BBB opening. GRE did not show bleeding. On Day 1 (D1) post sonication, the enhancement on post contrast T1-weighted imaging and the area with increased Ktrans on DCE imaging was smaller. There was a clearly-increased signal on T2-weighted imaging, and no bleeding on GRE. On Day 7 (D7) post sonication, there was no enhancement on T1-post contrast and DCE imaging, but GRE showed bleeding. B: Immediately after sonication, both T1-post contrast imaging and the DCE imaging showed BBB opening in the target area. At D1, the enhancement on T1-post contrast imaging and the area with increased DCE intensity became smaller, and by Day 7 there was no enhancement on T1-post contrast or DCE imaging. T2-weighted images and GRE did not show change at any of the three time points.

T1: T1-weighted imaging; T2: T2-weighted imaging; GRE: gradient-echo; DCE: dynamic contrast enhanced.

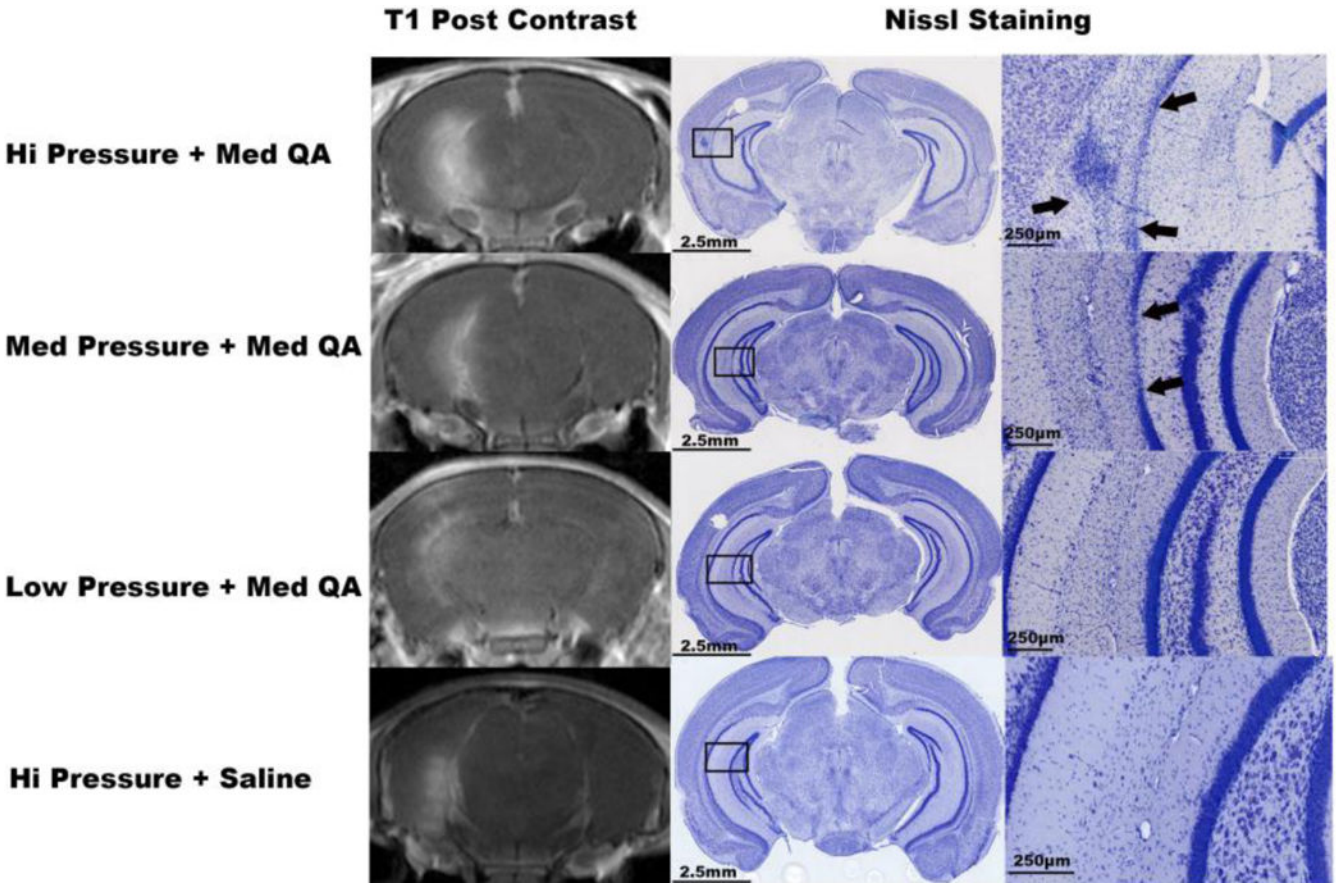

Fig. 3. BBB opening on MRI immediately after sonication and corresponding histologic damage induced by the high dosage of QA at Day 7 post-sonication.

Post contrast T1-weighted imaging (column 1) showed different sizes of enhancing areas: the higher the acoustic power, the larger the enhancing area. Low magnification Nissl-stained sections of the corresponding brain are shown in column 2, with black rectangles indicating the areas shown at higher magnification in column 3. Focal neuronal cell loss area (arrows) can be seen in the areas within the rectangles in the animals receiving High or Low Pressure sonication + QA. In contrast, the mice treated with either Low Pressure sonication + QA, or High Pressure sonication + saline did not show neuronal cell loss.

Table 1

Number of mice in each group showing BBB opening and or/edema

Acoustic power	High QA				Median QA				Low QA				Saline			
	BBB opening		Edema		BBB Opening		Edema		BBB Opening		Edema		BBB Opening		Edema	
	IM	D1	IM	D1	IM	D1	IM	D1	IM	D1	IM	D1	IM	D1	IM	D1
High	5/5	5/5	2/5	1/5	5/5	5/5	3/5	2/5	5/5	5/5	2/5	1/5	5/5	5/5	3/5	1/5
Median	5/5	5/5	2/5	0/5	5/5	5/5	0/5	2/5	5/5	5/5	1/5	0/5	5/5	5/5	1/5	0/5
Low	2/5	1/5	0/5	0/5	3/5	2/5	0/5	0/5	2/5	1/5	0/5	0/5	2/5	1/5	0/5	0/5

IM: immediately after sonication, D1: Day 1 after sonication

Table 2

BBB opening resulting from the different MRgFUS acoustic powers tested

	Hi Pressure	Med Pressure	Low Pressure
Intensity Ratio	1.82(1.48–1.94) *#	1.6(1.37–1.72)	1.38(1.32–1.53)
Enhanced Area (mm^2)	5(4–7.4) *	4.5(3.55–6.12) *	1.85(1.53–5.1)
Ktrans	0.27(0.2–0.32) **##	0.08(0.06–0.10)	0.065(0.06–0.07)

* P< 0.05

** P<0.01 versus Low FUS group

# P< 0.05

P<0.01

versus Medium FUS group. Intensity ratio, enhancement area,and Ktrans values were calculated from the data acquired immediately post FUS exposure.

Table 3

Lesion Area on Histology

	Hi QA(mm^2)	Med QA(mm^2)	Low QA(mm^2)	Saline
Hi Pressure	0.055±0.005 *	0.053±0.006	0.057±0.006 *	0
Med Pressure	0.037±0.005	0.038±0.006	0.01±0.004	0
Low Pressure	0	0	0	0

* 1 of the mice from the group showed bleeding.